Advancements in Antiviral Therapy: Favipiravir Sodium in Nasal Formulation

Priti Darne[1] · Shankar Vidhate[1] · Somesh Shintre[1] · Somnath Wagdare[2] · Dhiraj Bhamare[2] · Nisha Mehta[1] · Vishal Rajagopalan[1] · Sriram Padmanabhan[1]

Abstract

Favipiravir (FPV) is an Active Pharmaceutical Ingredient (API) known to have lower solubility in aqueous solvents. In the current study, efforts were made to generate a crystalline Favipiravir Sodium Salt (NaFPV) for enhanced solubility in aqueous media. The in-house generated NaFPV was characterized by NMR studies and its sodium content was determined by Flame Emission Spectroscopy (FES) as a confirmation of salt formation. Its solubility was determined where-in the solubility of NaFPV in water was about 100 times greater than FVP. FPV and NaFPV nasal spray formulations were prepared and its activity was determined against human coronavirus (hCoV) 229E strain. In the anti-hCoV assay as compared to FPV, NaFPV showed almost threefold higher anti-viral activity than its unmodified counterpart. Accelerated stability and spray pattern characteristics of both the formulations were studied. Interestingly, NaFPV showed higher physical stability during storage at conditions 40 ± 2 °C/ $75\% \pm 5\%$ RH. The nasal spray formulations of both FPV and NaFPV showed ideal plume geometry and spray pattern of acceptable specifications. Due to its improvement in terms of solubility, NaFPV will have higher rate and extent of absorption, and faster onset of the therapeutic effect and may appear to be a feasible alternative to regular favipiravir for use in solid dosage forms.

Keywords anti-covid activity · favipiravir · nasal spray formulations · solubility · stability studies

Abbreviations

FPV	Favipiravir
NaFPV	Favipiravir Sodium Salt
NMR	Nuclear Magnetic Resonance
BKC	Benzylkonium chloride
ACN	Acetonitrile
FBS	Fetal Bovine Serum
hCoV	Human Corona Virus

✉ Sriram Padmanabhan
   sriram.p@savaglobal.com

1   Innovation and Drug Discovery Division, Sava Healthcare Limited, Research Center, Block D1, Plot No. 17/6, MIDC, Chinchwad Pune-411019, India

2   Analytical Development Laboratory Division, Sava Healthcare Limited, Research Center, Block D1, Plot No. 17/6, MIDC, Chinchwad Pune-411019, India

Introduction

Favipiravir (FPV), developed by Toyoma Chemical Company Limited, Japan in 2002, was launched as an anti-influenza drug [1, 2]. FPV is a pyrazinecarboxamide derivative, that acts as a prodrug that is metabolized within cells to its active antiviral form, favipiravir-ribofuranosyl-5'-triphosphate (favipiravir-RTP) which in turn serves as a nucleotide analogue to selectively inhibit RNA-dependent RNA polymerase of the viruses and inhibit viral replication.

By the end of 2019, severe acute respiratory syndrome coronavirus 2 (SARS-CoV-2), affected more than 275 million people worldwide and caused nearly five million deaths, becoming a major public health issue by 2021. As the pandemic spread to Europe and no specific drugs available for treatment, drug repositioning was tried in hospitals, clinics with approvals from regulatory authorities and these drugs included lopinavir/ritonavir, remdesivir, favipiravir, ivermectin and tocilizumab [3]. Of these, remdesivir and favipiravir were more promising despite having side effects; although they are yet to be approved as the official anti-viral drug for SARS-CoV-2.

The EC_{50} of FPV for SARS-CoV-2 is found to be 61.88 μM as determined previously by in vitro studies [4]. To date, in several clinical cases FPV has received approval for emergency use in Italy, followed by its use in Japan, Russia, Ukraine, Uzbekistan, Moldova, Kazakhstan, Saudi Arabia, UAE, Turkey, Bangladesh, and Egypt [5]. In June 2020, Drugs Controller General of India (DCGI) approved the use of FPV for mild and moderate COVID-19 infections in India while it became a drug of choice in Thailand for prevention of healthcare-associated infection for COVID-19.

FPV is an RNA-dependent RNA polymerase inhibitor with strong activity against influenza virus. It has also shown activity in blocking the replication of other RNA viruses [6–8]. Approved in Japan for the management of emerging pandemic influenza infections in 2014 [5], several clinical trials have been conducted with FPV for tackling covid-19 infections. It was reported previously [9] that fever, cough, and dyspnea were improved significantly in FPV group as compared to lopinavir-ritonavir group. Reduction in viral load as well as improvement in clinical and radiological outcomes were observed in trials in China [10, 11]. As reported earlier, a multicentric, open-label, randomized controlled trial was conducted with covid confirmed adult patients in the UK, Brazil and Mexico received oral favipiravir (3600 mg on day 1 followed by 1600 mg daily for 9 days) [12]. The results indicated favipiravir not improving clinical outcomes in all patients but, patients younger than 60 years might have a beneficial clinical response [12]. Rattanaumpawan et al. [13] presented a retrospective observational study of 274 COVID-19 patients hospitalized at five hospitals in Thailand, of which 63 patients (23.0%) received FPV and reported promising effectiveness of FPV for treating COVID-19 patients. Safety and efficacy of FPV was proved in 150 adult patients with mild-to-moderate COVID-19 symptoms, where patients administered FPV showed significant improvement [14]. Following that, a multitude of studies emerged in India that started studying FPV activity against COVID-19 (3600 mg FPV on day 1 followed by 14 days of treatment of 1800 mg per day) enabling a clinical cure rate of more than 90% in the study subjects. [15]. Shinkai et al. [16] have demonstrated that FPV could be used for moderate COVID-19 pneumonia treatment. The percentage of patients who turned viral negative after a 14-day treatment of FPV was 77% as reported earlier [17]. FPV demonstrated rapid antiviral response against SARS-CoV-2 in a study as reported. [18].

Elevated serum uric acid is the common adverse effects (AE) observed during FPV treatment that turned back to normal after discontinuing the FPV therapy [19]. The other AE that is drug-related reported are elevated transaminase levels, diarrhea (1.4%), nausea (0.84%), abdominal pain (0.28%) and thrombocytopenia (0.28%) [20]. Since the dose requirement through the oral route is significantly high (26 g/person), it is possible to expect that the adverse events could be minimized by alternate dosage forms since it raises toxicity concerns and low patient compliance associated with a high pill burden for the vulnerable population, especially frail elderly and those with multi-comorbidity. Alternate dosage forms of FPV to the conventional tablets has been developed by several researchers since it enables ease in drug administration and improves patient compliance [21] where FPV was solubilized at 13 mg/mL using 0.14% poloxomer 188 at a pH of 5.7. The Indian regulatory agency has approved a FPV oral suspension of 100 mg/mL to overcome multiple tablets [22]. FPV has a characteristic high permeability but due to lower water solubility it has reduced effectiveness and bioavailability [23]. To address this issue of solubility solutions like favipiravir-encapsulated nano-emulsions as prospective carriers of drug delivery against COVID-19 have been developed [24] and use of super critical carbon dioxide (SC-CO$_2$) [25] where the solubility of FPV in SC-CO$_2$ varying from 0.004 to 2.618 g/L was obtained. The use of ethanol as a co-solvent with SC-CO$_2$ increased the solubility of FPV by 33% to what is achieved with SC-CO$_2$ alone [26]. Recent studies have successfully demonstrated the efficacy of a unique formulation of FPV as a dry powder inhaler and demonstrated its safety through inhalation studies in rats and human academic trials [27]. Hajibabaei et al. [28] demonstrated the potential of $(Zn(tren))^{2+}$ as a safe drug vehicle for making a soluble FPV entity where FPV is easily released and replaced by a Cl^- anion, or an H_2O molecule [28]. An inhalation solution of favipiravir of 2 mg/mL was developed and characterized recently [29]. Akbal-Dagistan et al. [30] developed a soft-mist inhaler with FPV (1, 2.5, 5 or 10 mg/kg in 1 mL saline) administered by inhalation within 2 min for 5 consecutive days that was diluted in saline. Shaik and co-workers [31] describe proliposomal powder formulation of FPV for pulmonary delivery by nebulization.

In this paper, we attempted making a nasal liquid formulation of favipiravir and also looked into the possibility of generating a salt form of favipiravir API since salt forms of newly developed APIs increase the API's solubility and therefore the bioavailability.

Materials and Methods

Chemicals and API

Favipiravir (Batch no: FIR0290820) was procured from Honour Labs, Telangana, India. Sodium carbonate, Sodium monophosphate, Sodium diphosphate was procured from SRL, India while methyl beta-cyclodextrin (Kleptose), Benzylkonium chloride (BKC), sodium chloride (NaCl), disodium Ethylene diamine tetra acetic acid (EDTA) was

from Merck, USA. Acetonitrile, Methanol, Orthophosphoric acid were of analytical grade, unless mentioned otherwise. Pump (cat # PUMP-140-VP3-CRIMP-20–43.5) was procured from Aptar Pharma, France. All the chemicals and reagents used were of analytical grade, unless mentioned otherwise.

In-house Synthesis of NaFPV

10gm of FPV was added to 200 mL methanol in a round bottom flask to make a suspension. The suspension was heated at 50–55 °C to get a clear solution. This solution was then added to sodium carbonate solution (3.4 g sodium carbonate in 20 mL deionized water). The mixture was heated at 50–55 °C for 5 min. Once, a yellow solid precipitation was observed, the content was cooled at room temperature. The slurry was then filtered through filter paper and washed with 10 mL methanol. The filtrered material was dried and yellow solid was obtained. The NaFPV synthesized was further characterized by Nuclear Magnetic Resonance (NMR) at ALR Labs, Hyderabad and sodium content was determined by Flame Emission Spectrophotometry (FES) at Ross Lifesciences Ltd., Pune.

Nasal Liquid Formulations of FPV and NaFPV

FPV solubility was achieved in 0.5 M sodium phosphate buffer of pH 6.8 containing 0.5% sodium carbonate and 6% beta-cyclodextrin at a concentration of 35 mg/mL. In the solubilized FPV solution, 0.25 mg/mL BKC, 0.5 mg/mL disodium EDTA and 9 mg/mL sodium chloride was added while stirring using a magnetic stirrer for 30 min. The clear, pale yellow formulation was kept for stability and other following parameters. Sodium FPV formulation of 35 mg/mL was prepared exactly by the same method as mentioned for FPV. The prepared formulations were aliquoted 10 mL each in a 15 mL glass bottles (clear and amber) fitted with stopper and seal and charged for stability at temperatures 0–8˚C and 25˚C with 60% Relative Humidity (RH), 30˚C with 75% RH and 40˚C at 75% RH as per the ICH guidelines for stability studies of pharmaceutical formulations. HPLC analysis for formulations by performing assay and related substances was carried for 0 day and 2 months. Suitable placebo formulation was made with all excipients without FPV/NaFPV. The formulations were stored in amber colored 15 mL glass bottles fitted with 140 μL Aptar pump.

For measuring viscosity, a Brookfield DV1 Viscometer was employed to assess the FPV and Na-FPV nasal spray samples taken after 2 months. Approximately 8 ml of the formulation was placed in a container, and a spindle attached to the instrument was immersed in the solution. Viscosity readings were measured in centipoise, with a torque of 0.3% at 100 rpm at 25 °C.

HPLC Analysis

For HPLC assay, 0.1% Orthophosphoric acid in water (pH 2.15) was used as buffer. The mobile phase Buffer: Acetonitrile (ACN) in the ratio of (75:25) % v/v was used for the assay. Chromatographic conditions were as follows: Column Intertsil ODS-C18, 250×4.6 mm, 5 μm. Detector wavelength—225 nm, Column temperature of 40 °C, Sampler temperature of 15 °C, Flow rate—1.0 mL/minute, Injection Volume—10 μl, Run time—10 min.

A mixture of water: methanol in ratio of 50:50% v/v as a diluent was prepared for standard and sample preparation. FPV standard was prepared in methanol and suitably diluted with methanol for HPLC analysis. Both the samples of the formulations and the standard were filtered through a 0.45 μm filter before injecting it for the HPLC analysis.

Related Substances (RS) Analysis Method for HPLC

For HPLC RS analysis, mobile phase A consisted of 0.1% orthophosphoric acid in water adjusting the pH to 3.0 ± 0.05 with Potassium hydroxide solution as buffer. Mobile phase B consisted of ACN: Water in the ratio of (80: 20) % v/v. The chromatographic conditions were as follow: Column—Purospher STAR, RP -18 end capped 3 μm, 250×4.6 mm or equivalent, detector wavelength—225 nm, Column temperature—35 °C, Sampler temperature—15 °C, Flow rate—0.7 mL/mL, Injection volume—10μL, run time—65 min.

A mixture of ACN: water in ratio of (50:50) % v/v was used as diluent for Standard and Sample preparation. A gradient program started with 90% of mobile phase A followed by 25%, 50%, 90% and 90% phase A at time points of 42, 50, 55 and 65 min respectively. The % mobile phase B at point 1 started with 10% mobile phase B and 75%, 50% 10 and 10% at 42, 50, 55 and 65 min respectively. Standard solution was prepared by dissolving 35 mg FPV in 100 mL of methanol ensuring complete dissolution. Standard, Placebo and Sample were filtered through 0.45 μm filter prior to injecting for HPLC analysis.

Cytotoxicity and Anti-hCoV Testing

Adherent cell lines MRC-5 fibroblasts (ATCC CCL-171) from human origin pertinent to coronavirus 229E, isolated from lung tissue were used for cytotoxicity and antiviral testing. The cell lines were maintained and propagated using EMEM with 10% FBS. The cytotoxicity and anti-viral testing was performed at Bhavan's Research Centre, Mumbai, India.

Cytotoxicity Assay

The FPV and NaFPV formulations were tested for cytotoxicity in MRC-5 cell line (ATCC CCL-171) susceptible to

coronavirus 229E utilizing the 3-(4,5-dimethylthiazol-2-yl)-2,5-diphenyltetrazolium bromide (MTT) assay. Freshly sub-cultured MRC-5 cells (Passsage # 7) were harvested and counted using the trypan blue dye exclusion test. The following day, the pre-seeded cells were exposed to 100 µL of the FPV, NaFPV formulation and placebo control using five-fold dilution scheme with concentrations ranging from 1000—0.0128 µg/mL in EMEM with 2% FBS performed in triplicates. Cell control wells (un-treated cells in 100 µL EMEM supplemented with 2% FBS) were maintained as controls during the assay. The plate was then incubated in a CO_2 incubator maintained at 37°C and 5% CO_2 for 5 days. Post-incubation, the plate was observed microscopically, and 20 µL MTT (5 mg/ mL) was added to each of the wells and the plate was re-incubated in a CO_2 incubator maintained at 37°C and 5% CO_2 for 3 h. After 3 h, the supernatant was discarded and 100 µL of DMSO was added to each well and the plate was re-incubate for 1 h the absorbance was measured at 490 nm with a reference measurement at 630 nm [32].

The CC_{50} (Cytotoxic Concentration showing 50% cell cytotoxicity/ viability) was calculated by using the formula,

$$CC_{50} value(mg/mL) = EXP((c - 50)/m); where : c = constant and m = slope of the equation$$

Cell Associated Antiviral Assay

The antiviral activity of FPV and NaFPV formualtions against human coronavirus (hCoV) 229E strain was evaluated using cell-based assays. Freshly sub-cultured MRC-5 cells were harvested and the cells were counted using the trypan blue dye exclusion test. 100 µL of the cell concentration (5×10^4 cells/mL) in EMEM supplemented with 10% FBS, was added to each well of a cell culture treated 96 well flat bottom plate. The plate was incubated in a CO_2 incubator maintained at 37°C and 5% CO_2. The following day, the cells were exposed to 100 µL of freshly prepared and titrated hCoV-22E virus adjusted to a concentration of 1000 PFU/mL in EMEM supplemented with 2% FBS. The plate was incubated in a CO_2 incubator maintained at 37°C and 5% CO_2 for 1 h to allow virus adsorption on to the cells. Post-virus adsorption, 100 µL of the prepared test product diluted following a five-fold dilution scheme were added to the cells infected with the virus in triplicates, i.e. three wells for each concentration range 200 µg/ mL to 0.0026 µg/mL). Virus control (virus exposed but untreated) and cell control (cells unexposed and un -treated with virus or the test products) wells were maintained in EMEM supplemented with 2% FBS as controls during the assay. The plate was incubated in a CO_2 incubator maintained at 37°C and 5% CO_2 for 5 days. Post-incubation, the plate was observed microscopically, following which the supernatant from the plate was

discarded and 100 µL of neutral red solution (50 µg/mL) prepared in EMEM supplemented with 2% FBS was added to all but three control wells which were used as blanks. The plate was re-incubated in a CO_2 incubator for 2 h. Post incubation, the supernatant from each well was discarded and the cell monolayers were carefully washed with 100 µL of DPBS. After washing, 100 µL of destaining solution (50% ethanol, 49% de-ionized water, 1% glacial acetic acid) was added to all the wells and incubated at room temperature for 15 min before measuring absorbance at 490 nm. The absorbance reading of the blank wells was subtracted from the test and the control wells and % inhibition calculated using the formula,

$$\%inhibition = (test/control)/100$$

A scatter plot of concentration vs % inhibition was plotted and a curve fitting (logarithmic trend line) along with Y intercept and equation. The IC_{50} (Inhibitory Concentration showing 50 % inhibition of virus cytopathic effect) was calculated by using the formula:

$$IC_{50} value(mg/mL) = EXP\{(c - 50)/m\} where : c = constant and m = slope of the equation$$

LC–MS Analysis

MS/MS system used was Shimadzu LCMS-8045 (model Nexera), which achieves both high sensitivity and ultra-high-speed detection, outfitted by heated electrospray ionization (ESI) probe. Mass range: m/z 2 to 2000 and Positive–negative ion polarity switching time: 5 ms was used for the Favipiravir formulation analysis. A 0.01 M ammonium acetate buffer at pH 2.5 was prepared by adding formic acid and used as mobile phase A. The mobile phase B consisted of (50:50 v/v of ACN: Water and the samples were diluted in a diluent composed of ACN: Water (50:50 v/v). The chromatographic conditions for LC–MS analysis of the Favipiravir formulation were as follows: Hypersil ODS C18 column (250×4.6 mm, 5 µm), detector wavelength set at 225 nm, column temperature maintained at 35 °C, and sampler temperature at 15 °C. The injection volume was 10 µL with the flow rate was set at 0.7 mL/min and a gradient elution was performed over 65 min as described in the RS method.

Characterization of Spray Pattern and Plume Geometry

Both the nasal spray formulations were subjected to spray pattern and plume geometry using the SprayVIEW NSP system (Proveris Scientific Cooperation, Marlborough, MA, USA). FPV and NaFPV nasal spray (0-day and 2 month stability sample) were shaken and primed four

times, followed by one test actuation before the measurement. The actuation was done upwards using the nasal spray devices with constant stroke length, compression velocity, and hold time. For spray-pattern measurements, a laser light, positioned 3 cm above the device tip in a horizontal position, was used and images captured using a high-speed digital camera while a vertically oriented laser sheet, along the long axis of the nasal spray device, was employed for plume geometry measurements wherein the plume was imaged from the side, directly above the device tip. All the images were captured at a 250 frames/s.

Characterization of Droplet Size Distribution

A Malvern Spraytec (Malvern Instruments Ltd., Westborough, MA, USA) was used to characterize the droplet-size distributions of FPV and NaFPV nasal spray. The 0 day both the nasal spray formulations were shaken and primed four times, followed by one test actuation before the measurement. The setup involves vertically mounting devices in an automated actuator system called SprayVIEW NSx, positioning them such that the actuator tip is 5 cm below a laser beam. The parameters controlling the actuator's movement or function are consistent with those used in other measurements involving plume geometry and spray-patterns. This setup ensures a standardized approach to conducting experiments or collecting data related to these measurements. Data were collected at 1000 Hz over 300 ms.

Results

Characterization of Sodium Favipiravir

The scheme followed for making sodium salt of Favipiravir is given in Fig. 1. Table I gives the properties of FPV and NaFPV on various parameters. It was interesting to observe that we could achieve an aqueous solubility of 120 mg/mL with NaFPV, as against 2 mg/mL for FPV, which was ~ 24-fold more than the native solubility of FPV. The viscosity of both the FPV and NaFPV nasal liquid formulations after 2 months was found to be within acceptable criteria. The incorporation of sodium in NaFPV was confirmed by NMR and FES analysis and the sodium content in NaFPV as determined by FES was found to be 12.40% against the theoretical calculated value of 12.84% which proves the formation sodium salt form of FPV (Table I).

1H NMR of NaFPV showed only three protons while in 1H NMR of FPV, four protons were observed. One proton of hydroxyl group at 13.40 ppm in FPV 1H NMR is absent in 1H NMR of NaFPV which suggests the formation of sodium salt of Favipiravir. Three distinct protons observed

in NaFPV 1H NMR, one aromatic proton at 7.88 ppm, one proton at 10.75 ppm which might be of proton of hydroxyl group of amide carbonyl due to amide iminol tautomerism, one proton at 7.21 ppm is proton attached to nitrogen of amide iminol form (Fig. 2A and B).

HPLC Analysis

In our current study, the nasal spray formulation of FPV showed 98.2% assay with a retention time (RT) of 4.6 min similar to standard FPV. After 30 days of storage as per ICH guidelines, conventional HPLC analysis indicated assay values of 101.8% at 2–8 °C, 97.1% at 25 °C, 99.4% at 30 °C, and 93.1% at 40 °C, suggesting some degradation at higher temperatures post 30 days. The retention times of the FPV and NaFPV remained constant i.e. 4.66 min as per the HPLC analysis (Figs. 3A and 3B respectively).

Cytotoxicity and Anti-hCoV Testing

Reports on its inability of FPV to viral clearance also exists [33], although several CT trials speak about the success in covid treatment. A recent study demonstrates the efficiency of a DPI formulation of FPV in covid treatment [34] and this study opened up the possibility of a new nasal spray formulation to fight against covid. In line with these findings, the cytotoxic concentrations (CC_{50}) of FPV and NaFPV were determined using MRC-5 cells. The CC_{50} values were found to be 3.63 mM (0.570 mg/mL) for FPV and 4.64 mM (0.835 mg/mL) for NaFPV. Subsequently, the half-maximal inhibitory concentrations (IC_{50}) against the human corona virus were identified, and therapeutic indices (TI) were calculated for both compounds, demonstrating their effectiveness in-vitro (Table II). Notably, the NaFPV formulation exhibited a 2.7 folds higher therapeutic index (TI) than the unmodified FPV.

Related Substances (RS) Analysis Method for HPLC

It is evident from the RS data that the number of impurities generated with the FPV nasal spray (Figs. 4A-4D) is several folds higher as compared to the single impurity generated with NaFPV NS which is evident from Figs. 5A-5D and Table III. The data showed the presence of a major peak at 156 mass (Fig. S1A) at time zero while after 2 months, there were many impurities generated which is shown in Fig. S1B in majorly 183.1 mass peak. This is identified as 6-ethoxy-3- hydroxypyrazine-2-carboxamide, a known impurity of Favipiravir. Such impurity generation is responsible for reduction of almost 50% FPV after 2 months storage in comparison to zero time (Fig. S1C versus Fig. S1D, peak of 9.479 min).

Spray Pattern and Plume Geometry

Spray pattern measurements are visualized as the cross-sectional area perpendicular to the axis of the spray while the plume geometry measurements that highlight differences in plume angle and width across actuators, as viewed from a direction parallel to the flow direction of the spray is shown in Figs. 6A-6E and 7A-7E for a representative sample. The width of the spray cone is a complementary measurement to the spray pattern diameter. The spray pattern images show similar spray pattern area for both the formulations. The FPV and NaFPV nasal spray formulations were evaluated for spray pattern uniformity at distances of 30 mm and 60 mm from the edge of the orifice. The ovality ratio values were found to be 1.098 and 1.198 respectively for FPV NS formulations (Fig. 6, panel A and Fig. 6, panel B) while panels D and E reflect the ovality ratio values for initial samples of NaFPV NS formulations at 30 mm and 60 mm distance as 1.223 and 1.198 respectively (Fig. 6, panels D and panel E). The ovality ratio (Dmax/Dmin) at these distances approached ideal values that are reflected by the images that appear more circular and symmetric. After a stability study of 60 days, our nasal spray maintained consistent performance with ovality ratios of 1.076, 1.255, 1.101 and 1.218 at 30 mm and 60 mm distance for FPV NS and NaFPV NS formulations respectively (Table IV and Fig. 7, panels A, B, D and E).

The plume angle of a nasal spray refers to the angle at which the spray is emitted from the device. A smaller plume angle means that the spray is emitted in a more focused or narrow cone, resembling a jet-like stream. Both the FPV and the NaFPV formulations show an average plume angle of 49° that aligns well with industry standards (45° to 60°), indicating efficient deposition in the nasal cavity for FPV NS and NaFPV NS formulation. Interestingly, this angle remained consistent ($\sim 50°$) after 2 months of stability testing, highlighting the robust quality of our formulation (Fig. 6, panel C and Fig. 7, panel F).

Droplet Size Distribution

Table IV shows the Dv10, Dv50, and Dv90 diameters, corresponding to droplet size relating to the 10%, 50%, and 90% percentile of droplet population on a volume basis and are in the range of 60–70 µm which is well within acceptable limits.

Discussion

Approximately 12–15% difference in peak area was seen between FPV and NaFPV by HPLC and this difference matches with the molecular weight difference between FPV

Fig. 1 Schematic representation of process followed for making sodium salt of favipiravir
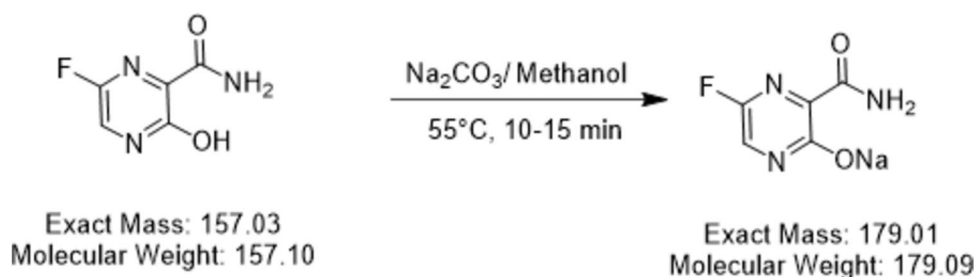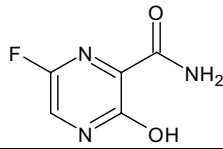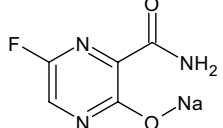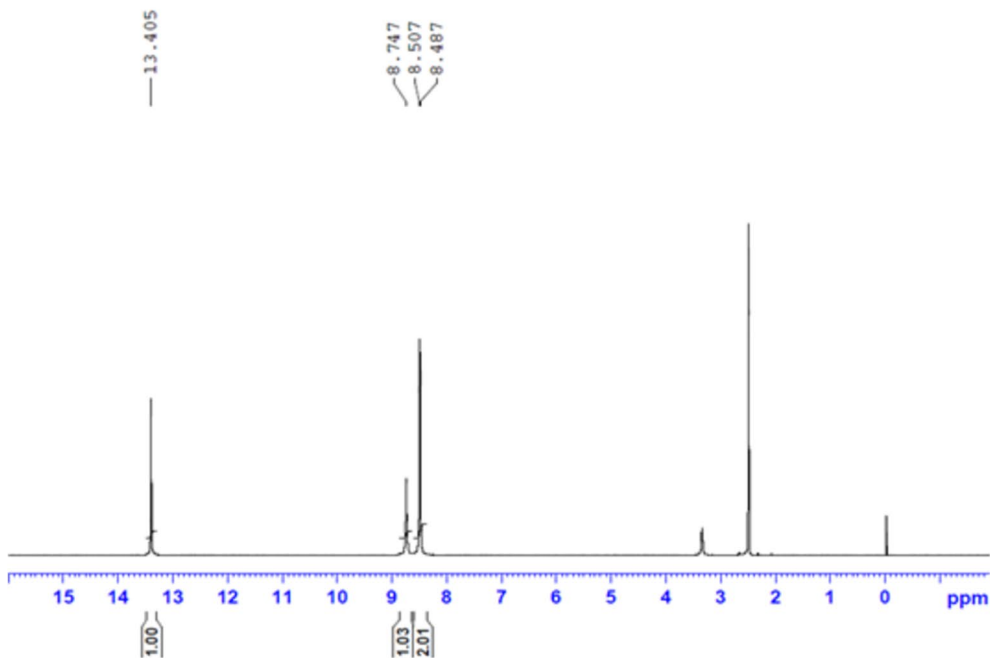
Na$_2$CO$_3$/ Methanol
55°C, 10-15 min

Exact Mass: 157.03
Molecular Weight: 157.10

Exact Mass: 179.01
Molecular Weight: 179.09

Table I Favipiravir (FPV) & Sodium Favipiravir (NaFPV) Comparison Data

Compound	Formula and CAS No	Sodium Content	Structure	M_w (g/Mol)	HPLC Data	λ max (nm)	Viscosity of NS formulations (cp)	Sodium content
FPV	C$_5$H$_4$FN$_3$O$_2$ 259793-96-9	Not applicable		157	Retention Time-4.7 min Purity- 99.9 %	324 nm in Methanol	1.5	Nil
NaFPV	C$_5$H$_3$FN$_3$NaO$_2$ Not applicable	12.4% (Theoretical 12.84%)		179	Retention Time-4.7 min Purity- 99.9 %	361 nm in Water	1.5	12.40%

Fig. 2 1H NMR Spectra of FPV and NaFPV API Panel **A** represents NMR spectra of FPV while Panel **B** represent NMR spectra of NaFPV

and NaFPV. The achievement of 120 mg NaFPV/mL is the highest solubility of FPV achieved in water and is hitherto unreported. The solubility of FPV has been reported to be in the range of 2.29 mg/mL [35] and 4.48 to 8.5 mg/mL [36]. Several efforts on modified formulations of FPV have been reported. These include strategies of co-crystallization with theophylline [35], complexation with naturally occurring macromolecules [37], encapsulation using super critical fluids (SCF) [25, 26], biodegradable nanoemulsions [24] etc. with moderate increase in solubility.

Nasal and pulmonary delivery systems target the delivered dose of the drug directly to the site of drug action and are non-invasive routes of administration [38] and since lung and nasal cavity have a low drug metabolizing environment, and drugs intended for these sites bypasses the first-pass

metabolism, this delivery platform appears to be an attractive alternative [39]. Therefore, our attempt was to prepare nasal spray (NS) formulations of both FVP and NaFPV.

Since it was essential to understand if the prepared NS formulations are biologically active, an in-vitro anti-hCoV activity was carried out using MRC5 cell-line (ATCC-CCL- 171), a cell line that is susceptible to hCoV-229 strain (ATCC VR-740) of the human corona virus. The higher TI of NaFPV over FPV for its antiviral activity against corona virus, could be attributed to its higher solubility over FPV in MRC5 cells leading to improved permeability and bioavailability for enhanced efficacy. The observation of almost three fold higher anti-hCoV activity of the NaFPV assumes critical importance since it might reduce the requirement of FPV dose to one third, which is currently very high (almost
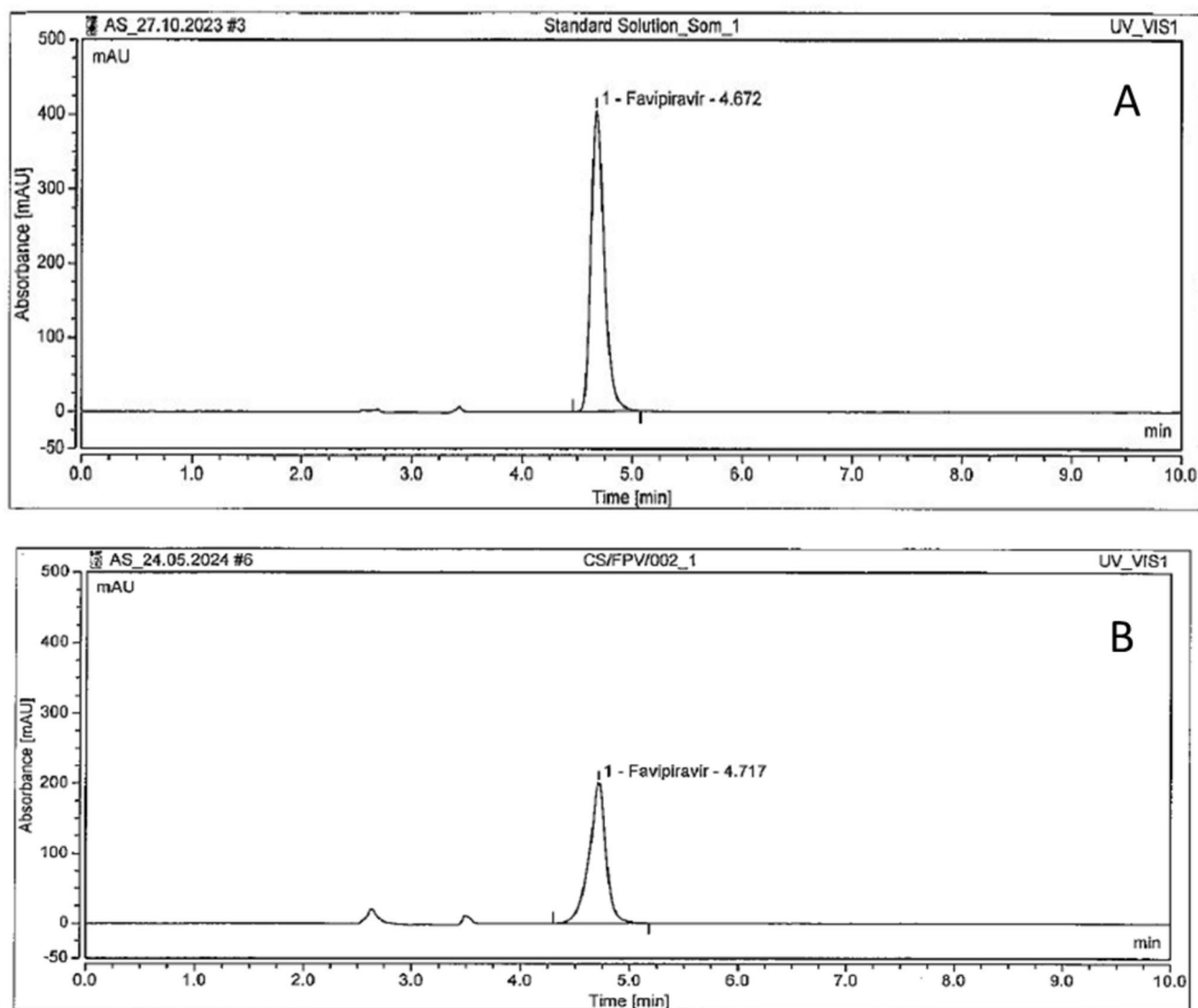

Fig. 3 Panel A shows the HPLC chromatogram of Favipiravir. Note the RT of 4.67 for a 1 ppm solution, panel B shows the HPLC chromatogram of Na-FPV with a RT of 4.67 min

26 g/person) for 14 days of treatment and might prevent adverse side- effects seen with FPV.

Non-invasive routes of drug administration like nasal are highly preferred as the drug is delivered directly at the site of infection [40, 41]. To ensure effective aerosolization, we studied the plume geometry and spray pattern analysis of FPV NS formulation, that are established techniques used in optimizing orally inhaled and nasal spray products (OIN-DPs) regulated since 1998. Spray Characteristics of the two different Formulations (Table IV) presents spray characteristics including spray patterns, plume geometries, and droplet-size distributions of each of the formulations of two different time points is represented. Spray patterns were characterized

Table II Anti-covid activity of Favipiravir and NaFPV NS Formulations

Active	CC$_{50}$ (mg/mL)	Antiviral Activity	
		Parameters	hCoV-229 E (ATCC VR-740)
FPV	0.570	IC$_{50}$ (mg/mL)	0.000861
		TI*	662.02
NaFPV	0.835	IC$_{50}$ (mg/mL)	0.000454
		TI*	1839.20

CC50 (Concentration showing 50% cytotoxicity/ viability): Determined by fitting logarithmic trend line to the data

IC50 (Concentration showing 50% inhibition): Determined by fitting logarithmic trend line to the data

TI Therapeutic Index (CC50 / IC50)

by the minimum (Dmin) and maximum (Dmax) spray diameters, ovality (Dmax/Dmin), and the spray area while plume geometries were characterized by the plume angle and the plume width values. The data indicates compliances of specifications for both FPV NS and NaFPV NS and supports values demonstrated for optimal spray performance reported for other NS products [42].

Droplet size distributions (DSDs) were characterized by the median (Dv50), and the 10th (Dv10) and 90th (Dv90) percentiles of the cumulative undersize distribution. The DSD of a nasal spray significantly influences the in-vivo deposition of the drug in the nasal cavity and is influenced by the actuation parameters of the device, formulation should be such that median droplet size is between 30 and 120 µm. If the droplets are larger than 120 µm, the deposition takes place mainly in the anterior parts of the nose, and if the droplets are too small it will reach the lungs which are not the intended site for nasal spray formulations [40]. Our data reflects clearly that the formulations developed have DSD well within the intended range and hence would be efficacious. The order of parameters having the greatest to least impact on the nasal posterior deposition (PD) of the drug is shown as cone angle ≫ plume ovality ≫ characteristic droplet size ≫ velocity ≫ size distribution uniformity constant [42] and our results supports these observations.

Regarding assessments of stability of favipiravir in the nasal spray formulations, HPLC analysis revealed susceptibility of FPV to oxidation and formation of impurities. Previous studies, such as those by Abdallah et al. [43] have detailed degradation pathways under alkaline and
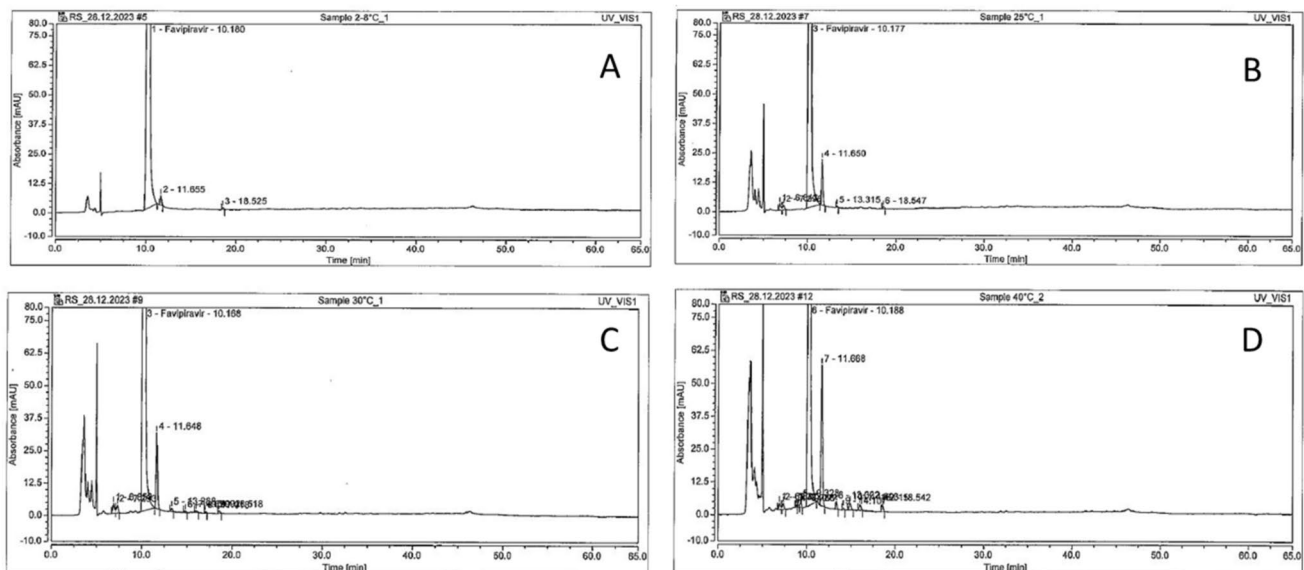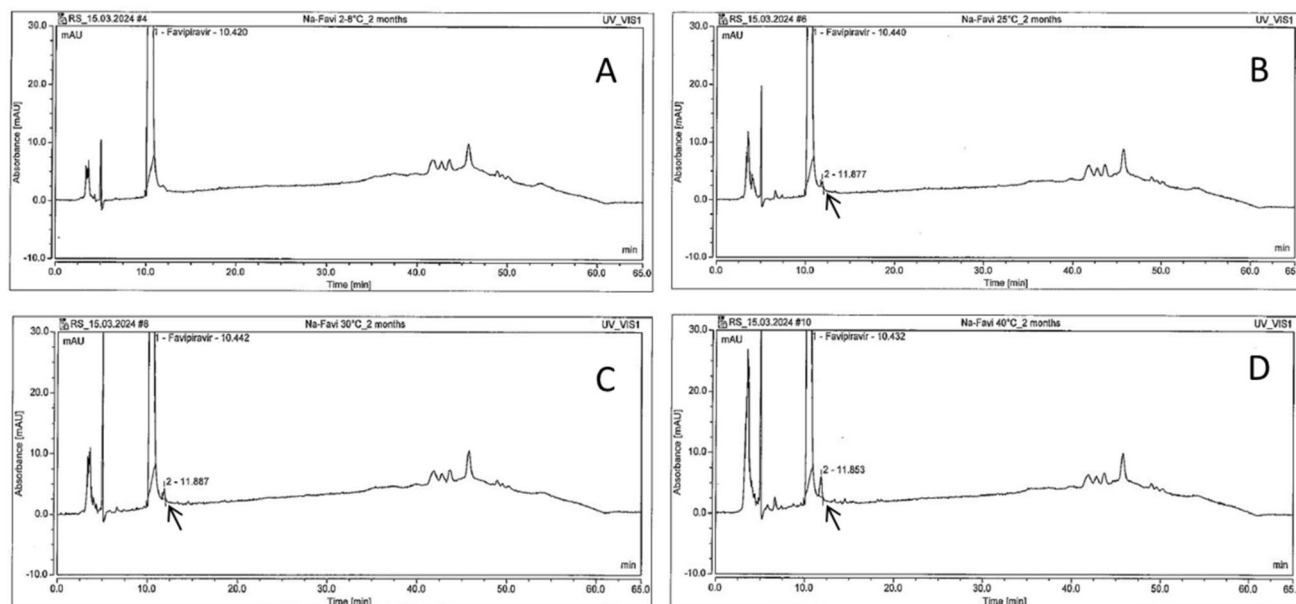

Fig. 4 HPLC chromatograms of FPV NS formulation after 2 months. Panel **A** at 2–8 °C sample, panel **B** at 25 °C {60% Relative Humidity (RH)}, panel **C** at 30 °C {70% Relative Humidity (RH)} and panel **D** at 40 °C{70% Relative Humidity (RH)}. Note the pronounced peak of an impurity at 11.85 min at all temperatures

Fig. 5 HPLC chromatograms of NaFPV NS formulation after 2 months. Panel **A** at 2–8 °C sample, panel **B** at 25 °C {60% Relative Humidity (RH)}, panel **C** at 30 °C {70% Relative Humidity (RH)} and panel **D** at 40 °C {70% Relative Humidity (RH)}

Table III Impurity Peaks Profile of FPV and NaFPV Ns Formulations After 60 Days of Stability Charging

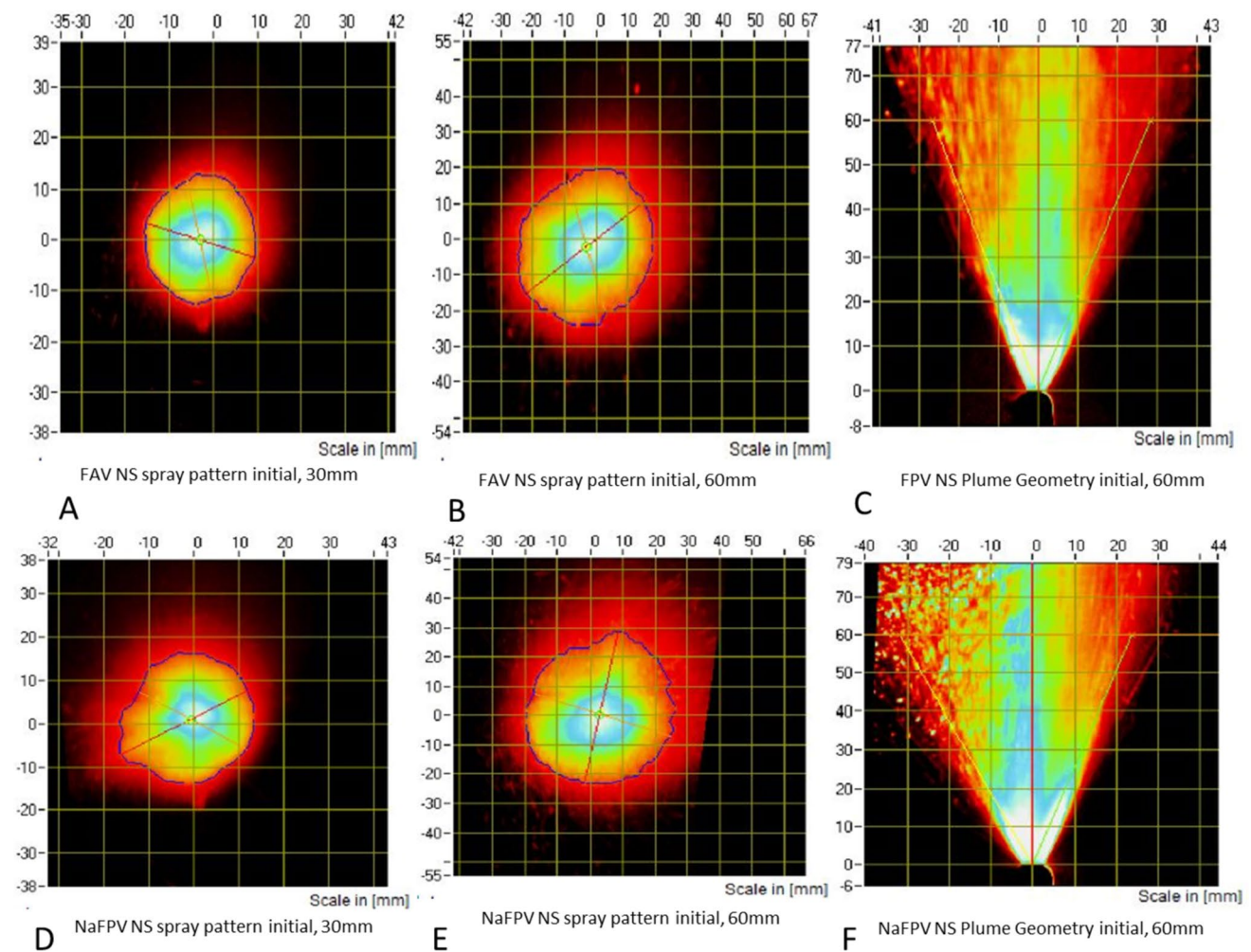| Stability Condition	FPV NS formulation impurities after 60 days by RS HPLC		NaFPV NS formulation impurities after 60 days by RS HPLC	
	Impurities (RTs)	Percentage (%)	Impurities (RTs)	Percentage (%)
2–8 °C	11.65 min	0.113	Nil	NA
	18.53 min	0.036		
25 °C (60% RH)	6.84 min	0.117	11.89 min	0.038
	7.29 min	0.096		
	11.65 min	0.580		
	13.30 min	0.025		
	18.55 min	0.040		
30 °C(70% RH)	6.85 min	0.160	11.89 min	0.068
	7.29 min	0.139		
	11.65 min	0.901		
	13.30 min	0.049		
	14.82 min	0.027		
	15.99 min	0.031		
	17.02 min	0.018		
	18.50 min	0.049		
40 °C(70% RH)	6.88 min	0.066	11.85 min	0.038
	7.31 min	0.065		
	8.80 min	0.028		
	9.32 min	0.082		
	11.66 min	1.927		
	13.32 min	0.101		
	14.10 min	0.038		
	14.88 min	0.152		
	16.00 min	0.136		
	18.52 min	0.127		

Fig. 6 The time-averaged composite images for spray pattern of FPV NS formulation of day 0 samples at 30 mm and 60 mm distance from the edge of the orifice is shown in panels **A** and **B** respectively with the ovality ratio values of 1.098 and 1.205 respectively while panels **D** and **E** reflect the ovality ratio values for initial samples of NaFPV NS formulations at 30 mm and 60 mm distance as 1.194 and 1.201 respectively. Effect of actuation velocity (80 mm/s) on the plume geometry of FPVNS and NaFPV NS formulations at day zero is depicted in panels **C** and **F** respectively. Note the plume angle of 50.2° and 49.7° for FPV and NaFPV formulations respectively, which are well within specified limits. (The force limits were maintained as contact force of 0.3 kg and the end of stroke force of 6.0 kg, other settings included laser height of 13.5 cm and plume orientation of 90 º acceleration = 7000 mm/s2, and hold time = 200 ms)

oxidizing conditions, identifying major degradants with distinct molecular weights. The stability data of our nasal spray formulations support the observations that salts offer stability to formulations and improves other pharmaceutical properties of drugs, such as stability, hygroscopicity, ease of manufacturing, and pharmaceutical processing [44, 45]. Since the number of impurities generated with the FPV NS formulation was significantly higher than its counter NaFPV, we proceeded with LC–MS analysis of Favipiravir NS alone and determine the specific impurity 6-ethoxy-3-hydroxypyrazine-2-carboxamide. Isolation and characterization studies of such impurities are in progress and will be discussed elsewhere.

Conclusion

Salt formation approaches have been widely adopted to increase solubility and in turn the dissolution rate of a drug. Commonly used salts such as hydrochlorides and sodium have advantages over other salt-forming moieties due to their low molecular weight and low toxicity, hence the current study assumes its critical importance. However, other salt forms like mesylate may sometimes offer advantages such as higher solubility and bioavailability [46] and could also be tested with FPV, in future. It is tempting to speculate that such a strategy could potentially reduce the dose of FPV required for viral clearance.
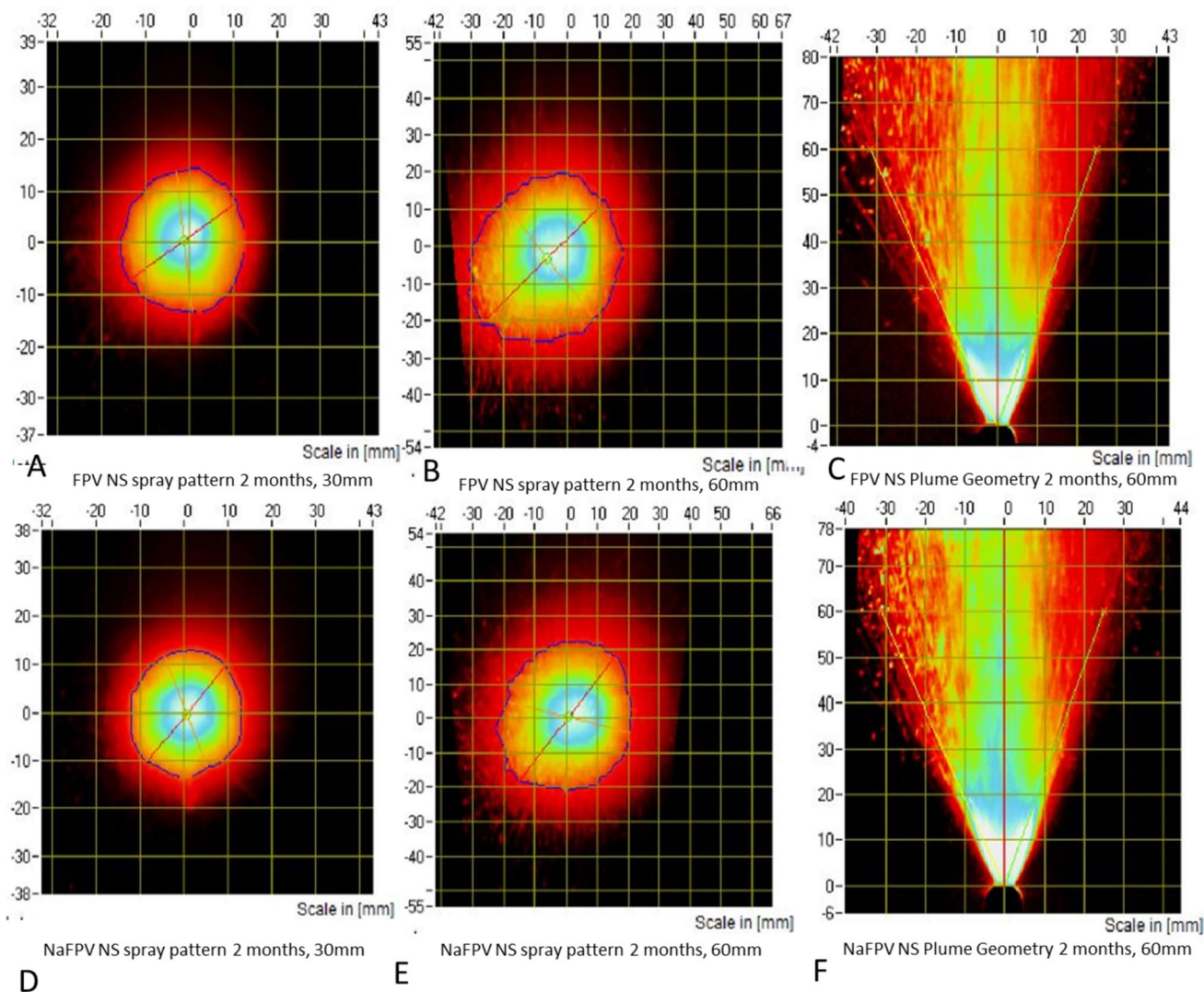
Fig. 7 The time-averaged composite image for spray pattern of FPV NS formulations of 2 month samples at 30 mm and 60 mm distance from the edge of the orifice is shown in panels **A** and **B** respectively with the ovality ratio values of 1.076 and 1.209 respectively while for NaFPV NS, the ovality ratio values were 1.087 and 1.218 respectively (panels **D** and **E**). Effect of actuation velocity (80 mm/s) on the plume geometry of FPVNS and NaFPV NS formulations of 2 months samples is depicted in panels **C** and **F** respectively. Note the plume angle of 50.2° and 49.7° for FPV and NaFPV formulations respectively, which are well within specified limits. (The force limits were maintained as contact force of 0.3 kg and the end of stroke force of 6.0 kg, other settings included laser height of 13.5 cm and plume orientation of 90 ° acceleration = 7000 mm/s2, and hold time = 200 ms)

Table IV Spray Pattern AND Plume Geometry Table for Favipiravir and Na-Favipiravir Nasal Spray

Formulation		30 mm distance					60 mm distance						
		Spray Pattern		DSD (μm)			Spray Pattern		Plume Geometry		DSD (μm)		
		Area (mm^2)	Ovality	D10	D50	D90	Area (mm^2)	Ovality	Angle (deg)	Width (mm)	D10	D50	D90
Favipiravir	Fresh	501.5	1.098	12.89	29.89	71.14	1433.1	1.205	49.2	54.9	16.39	32.26	60.46
	2 months	618.7	1.076				1677.2	1.209	50.5	56.7			
Na-Favipiravir	Fresh	696.6	1.194	13.05	30.19	70.01	1728.1	1.201	49.6	55.6	15.55	32.26	62.68
	2 months	534.3	1.087				1490.3	1.218	49.9	55.9			

Drug stability is affected adversely if a counter ion for salt formation is not chosen carefully chosen. This is because improper salt counter ions are known to cause degradation products with different biological activity, and therefore, they need to be avoided for further development. We observe that the sodium counter ion for FPV is a right choice since it increases solubility, enhances anti-hCoV activity and hence minimal degradation products when charged on stability. Since Favipiravir has proven efficacy against a broad range of human influenza viruses, including arenaviruses, bunyavirus, filovirus, westnile virus, phleboviruses, hantaviruses, flaviviruses, Western equine encephalitis virus, noroviruses, and Ebola virus, Lassa virus, Rift Valley fever virus, hemorrhagic fever arenavirus, Chikungunya virus, and Norovirus [5, 47–49], its salt version as described here, could be explored for further research. Favipiravir is also reported to introduce nucleotide mutations into the hepatitis A virus genome and work as an antiviral against HAV infection [50], it remains to be seen if such properties stay with the sodium salt of Favipiravir too. Converting a drug into its salt form is reported to increase its chemical stability, render the complex easier to administer and allow manipulation of the agent's pharmacokinetic profile [45]. Since the ionic drug salts exhibit variability in absorption, pharmacokinetics, drug action and excretion, hence the bioequivalence of the salt form of a drug is higher than the parent molecule. The chemical properties such as log P (partition coefficient), pK_a (dissociation constant) and melting point of the API due to salt formation will influence the behavior of the parent drug in the body through alterations in drug solubility, dissolution and stability and will be discussed elsewhere.

Data Availability All the data required is already within the manuscript. Additional data is provided in supplementary document.

Declarations

Conflict of Interest The authors declare no conflicts of interest.

References

1. Furuta Y, Takahashi K, Fukuda Y, Kuno M, Kamiyama T, Kozaki K, et al. In vitro and in vivo activities of anti-influenza virus compound T-705. Antimicrob Agents Chemother. 2002;46(4):977–81. https://doi.org/10.1128/aac.46.4.977-981.2002.

2. Łagocka R, Dziedziejko V, Kłos P, Pawlik A. Favipiravir in therapy of viral Infections. J Clin Med. 2021;10(2)273 https://doi.org/10.3390/jcm10020273.

3. Scavone C, Brusco S, Bertini M, Sportiello L, Rafaniello C, Zoccoli A, et al. Current pharmacological treatments for COVID-19: What's next? Br J Pharmacol. 2020;177(21):4813–24. https://doi.org/10.1111/bph.15072.

4. Wang M, Cao R, Zhang L, Yang X, Liu J, Xu M, et al. Remdesivir and chloroquine effectively inhibit the recently emerged novel coronavirus (2019-nCoV) in vitro. Cell Res. 2020;30(3):269–71. https://doi.org/10.1038/s41422-020-0282-0.

5. Agrawal U, Raju R, Udwadia ZF. Favipiravir: A new and emerging antiviral option in COVID-19. Med J Armed Forces India. 2020;76(4):370–6. https://doi.org/10.1016/j.mjafi.2020.08.004.

6. Kulkarni P, Padmanabhan S. A novel property of hexokinase inhibition by Favipiravir and proposed advantages over Molnupiravir and 2 Deoxy D glucose in treating COVID-19. Biotechnol Lett. 2022;44(7):831–43. https://doi.org/10.1007/s10529-022-03259-6.

7. Furuta Y, Komeno T, Nakamura T. Favipiravir (T-705), a broad spectrum inhibitor of viral RNA polymerase. Proc Japan Acad Series B. 2017;93(7):449–63. https://doi.org/10.2183/pjab.93.027.

8. Delang L, Abdelnabi R, Neyts J. Favipiravir as a potential countermeasure against neglected and emerging RNA viruses. Antiviral Res. 2018;153:85–94. https://doi.org/10.1016/j.antiviral.2018.03.003.

9. Tabarsi P, Vahidi H, Saffaei A, Hashemian SMR, Jammati H, Daraei B, et al. Favipiravir effects on the control of clinical symptoms of hospitalized COVID-19 cases: An experience with Iranian formulated dosage form. Iran J Pharm Res. 2021;20(4): e124266. https://doi.org/10.22037/ijpr.2021.115510.15401.

10. Cai Q, Yang M, Liu D, Chen J, Shu D, Xia J, et al. Experimental treatment with favipiravir for COVID-19: An open-label control study. Engineering (Beijing). 2020;6(10):1192–8. https://doi.org/10.1016/j.eng.2020.03.007.

11. Chen C, Zhang Y, Huang J, Yin P, Cheng Z, Wu J, et al. Favipiravir versus arbidol for clinical recovery rate in moderate and severe Adult COVID-19 patients: A prospective, multicenter, open-Label, randomized controlled clinical trial. Front Pharmacol. 2021;12: 683296. https://doi.org/10.3389/fphar.2021.683296.

12. Shah PL, Orton CM, Grinsztejn B, Donaldson GC, Crabtree Ramírez B, Tonkin J, et al. Favipiravir in patients hospitalised with COVID-19 (PIONEER trial): a multicentre, open-label, phase 3, randomised controlled trial of early intervention versus standard care. Lancet Respir Med. 2023;11(5):415–24. https://doi.org/10.1016/s2213-2600(22)00412-x.

13. Rattanaumpawan P, Jirajariyavej S, Lerdlamyong K, Palavutitotai N, Saiyarin J. Real-world experience with favipiravir for treatment of COVID-19 in Thailand: Results from a multicenter

observational study. medRxiv. 2020:2020.06.24.20133249. https://doi.org/10.1101/2020.06.24.20133249.

14. Udwadia ZF, Singh P, Barkate H, Patil S, Rangwala S, Pendse A, et al. Efficacy and safety of favipiravir, an oral RNA-dependent RNA polymerase inhibitor, in mild-to-moderate COVID-19: A randomized, comparative, open-label, multicenter, phase 3 clinical trial. Inter J Infect Dis. 2021;103:62–71. https://doi.org/10.1016/j.ijid.2020.11.142.

15. Joshi S, Parkar J, Ansari A, Vora A, Talwar D, Tiwaskar M, et al. Role of favipiravir in the treatment of COVID-19. Int J Infect Dis. 2021;102:501–8. https://doi.org/10.1016/j.ijid.2020.10.069.

16. Shinkai M, Tsushima K, Tanaka S, Hagiwara E, Tarumoto N, Kawada I, et al. Efficacy and safety of favipiravir in moderate COVID-19 pneumonia patients without oxygen therapy: A randomized, phase III clinical trial. Infect Dis Ther. 2021;10(4):2489–509. https://doi.org/10.1007/s40121-021-00517-4.

17. Lou Y, Liu L, Yao H, Hu X, Su J, Xu K, et al. Clinical outcomes and plasma concentrations of Baloxavir, Marboxil and Favipiravir in COVID-19 patients: An exploratory randomized, controlled trial. Eur J Pharm Sci. 2021;157: 105631. https://doi.org/10.1016/j.ejps.2020.105631.

18. Ivashchenko AA, Dmitriev KA, Vostokova NV, Azarova VN, Blinow AA, Egorova AN, et al. AVIFAVIR for treatment of patients With moderate coronavirus disease 2019 (COVID-19): Interim results of a phase II/III multicenter randomized clinical trial. Clin Infect Dis. 2021;73(3):531–4. https://doi.org/10.1093/cid/ciaa1176.

19. Papp H, Lanszki Z, Keserű GM, Jakab F. Favipiravir for the treatment of COVID-19 in elderly patients-what do we know after 2 years of COVID-19? Geroscience. 2022;44(3):1263–8. https://doi.org/10.1007/s11357-022-00582-8.

20. Ergür F, Yıldız M, Şener MU, Kavurgacı S, Ozturk A. Adverse effects associated with favipiravir in patients with COVID-19 pneumonia: a retrospective study. Sao Paulo Med J. 2022;140(3):372–7. https://doi.org/10.1590/1516-3180.2021.0489.R1.13082021.

21. Tuesuwan B, Mueannoom W, Jamnongtanachot P, Khunvichai A, Pavitrapok C, Wongpakdee K, et al. Basis to aid crisis: Favipiravir oral solution for hospital compounding during COVID-19 drug shortage. J Pharm Sci. 2023;112(2):610–7. https://doi.org/10.1016/j.xphs.2022.10.026.

22. Patel R, Dube A, Solanki R, Khunt D, Parikh S, Junnuthula V, et al. Structural elucidation of alkali degradation impurities of favipiravir from the oral suspension: UPLC-TQ-ESI-MS/MS and NMR. Molecules. 2022;27:5606. https://doi.org/10.3390/molecules27175606.

23. Moshikur RM, Ali MK, Wakabayashi R, Moniruzzaman M, Goto M. Favipiravir-based ionic liquids as potent antiviral drugs for oral delivery: Synthesis, solubility, and pharmacokinetic evaluation. Mol Pharm. 2021;18(8):3108–15. https://doi.org/10.1021/acs.molpharmaceut.1c00324.

24. Abd El-Kodous M, Samuel Oluwaseun O, Morsi M, El-Sayyad G. Nanomaterial-based drug delivery systems as promising carriers for patients with COVID-19. RSC Adv. 2021;11:26463. https://doi.org/10.1039/d1ra04835j.

25. Sajadian SA, Ardestani NS, Esfandiari N, Askarizadeh M, Jouyban A. Solubility of favipiravir (as an anti-COVID-19) in supercritical carbon dioxide: An experimental analysis and thermodynamic modeling. J Supercrit Fluids. 2022;183: 105539. https://doi.org/10.1016/j.supflu.2022.105539.

26. Rojas A, Sajadian SA, López-de-Dicastillo C, Ardestani NS, Aguila G, Jouyban A. Improving and measuring the solubility of favipiravir and montelukast in SC-CO(2) with ethanol projecting their nanonization. RSC Adv. 2023;13(48):34210–23. https://doi.org/10.1039/d3ra05484e.

27. Vaidya V, Nirhali S, Agarwal R. Proof of concept study to evaluate the safety and effectiveness of a novel favipiravir dry powder inhalation formulation in subjects with SARS-COV-2 infection. Innov Pharm Pharmacother. 2021;9(3):48–58. https://doi.org/10.31690/ipp.2021.v09i03.002.

28. Hajibabaei F, Sanei Movafagh S, Salehzadeh S, Gable R. A tris(2-aminoethyl)amine-based zinc complex as a highly water-soluble drug carrier for the anti-COVID-19 drug favipiravir: a joint experimental and theoretical study. Dalton transactions (Cambridge, England : 2003). 2023;52. https://doi.org/10.1039/d3dt00256j.

29. Pekoz AY, AkbalDagistan O, Fael H, Culha M, Erturk A, Basarir NS, et al. Pulmonary delivery of favipiravir inhalation solution for COVID-19 treatment: in vitro characterization, stability, in vitro cytotoxicity, and antiviral activity using real time cell analysis. Drug Deliv. 2022;29(1):2846–54. https://doi.org/10.1080/10717544.2022.2118398.

30. Akbal-Dagistan O, Sevim M, Sen LS, Basarir NS, Culha M, Erturk A, et al. Pulmonary delivery of favipiravir in rats reaches high local concentrations without causing oxidative lung injury or systemic side effects. Pharmaceutics. 2022;14(11):2375. https://doi.org/10.3390/pharmaceutics14112375.

31. Shaik NB, Lakshmi PK, Basava Rao VV. Formulation and evaluation of favipiravir proliposomal powder for pulmonary delivery by nebulization. Inter J Pharma Res Allied Sci. 2022;11(2):36–44. https://doi.org/10.51847/4McfhPccXs.

32. Leneva I, Kartashova N, Poromov A, Gracheva A, Korchevaya E, Glubokova E, et al. Antiviral activity of Umifenovir in vitro against a broad spectrum of coronaviruses, including the novel SARS-CoV-2 virus. Viruses. 2021;13(8):1665. https://doi.org/10.3390/v13081665.

33. Luvira V, Schilling WHK, Jittamala P, Watson JA, Boyd S, Siripoon T, et al. Clinical antiviral efficacy of favipiravir in early COVID-19 (PLATCOV): an open-label, randomised, controlled, adaptive platform trial. BMC Infect Dis. 2024;24(1):89. https://doi.org/10.1186/s12879-023-08835-3.

34. Padmanabhan S, Jadhav VR. Dry powder inhalation (dpi) formulation. IN 418700 B. 2023.

35. Wong SN, Weng J, Ip I, Chen R, Lakerveld R, Telford R, et al. Rational development of a carrier-free dry powder inhalation formulation for respiratory viral infections via quality by design: A drug-drug cocrystal of favipiravir and theophylline. Pharmaceutics. 2022;14(2):300.

36. Timur S, AtaŞOĞLu M, ÖNer Y, Karabulut T, Eroglu H. In vitro studies for BCS classification of an antiviral agent, Favipiravir. J Res Pharm. 2021;25(6):944–52. https://doi.org/10.29228/jrp.91.

37. Morozova MA, Tumasov VN, Kazimova IV, Maksimova TV, Uspenskaya EV, Syroeshkin AV. Second-order scattering quenching in fluorescence spectra of natural humates as a tracer of formation stable supramolecular system for the delivery of poorly soluble antiviral drugs on the example of mangiferin and favipiravir. Pharmaceutics. 2022;14(4). https://doi.org/10.3390/pharmaceutics14040767.

38. Thwala L, Preat V, Csaba N. Emerging delivery platforms for mucosal administration of biopharmaceuticals: A critical update on nasal, pulmonary and oral routes. Expert Opin Drug Deliv. 2016;14. https://doi.org/10.1080/17425247.2016.1206074.

39. Ghadiri M, Young PM, Traini D. Strategies to enhance drug absorption via nasal and pulmonary routes. Pharmaceutics. 2019;11(3):113. https://doi.org/10.3390/pharmaceutics11030113.

40. Kulkarni V, Shaw C. Formulation and characterization of nasal sprays. An examination of nasal spray formulation parameters and excipients and their influence on key in vitro tests. Inhalation. 2012. https://www.inhalationmag.com/wp-content/uploads/pdf/inh_20120601_0010.pdf. Accessed 13 Aug 2024.

41. Thorat S. Formulation and product development of nasal spray: an overview. Scholars J Appl Med Sci. 2016;4(08):2976–85. https://doi.org/10.36347/sjams.2016.v04i08.048.

42. Kolanjiyil AV, Walenga R, Babiskin A, Golshahi L, Hindle M, Longest W. Establishing quantitative relationships between changes in nasal spray in vitro metrics and drug delivery to the posterior nasal region. Int J Pharm. 2023;635: 122718. https://doi.org/10.1016/j.ijpharm.2023.122718.

43. Abdallah IA, El-Behairy MF, Ahmed RM, Fayed MAA. The anti-COVID-19 drug Favipiravir: Degradation, method development, validation, NMR/LC-MS characterization, and in-vitro safety evaluation. Chem Zvesti. 2022;76(10):6415–26. https://doi.org/10.1007/s11696-022-02327-5.

44. Neusaenger AL, Yao X, Yu J, Kim S, Hui HW, Huang L, et al. Amorphous drug-polymer salts: Maximizing proton transfer to enhance stability and release. Mol Pharm. 2023;20(2):1347–56. https://doi.org/10.1021/acs.molpharmaceut.2c00942.

45. Patel A, Jones S, Ferro A, Patel N. Pharmaceutical salts: A formulation trick or a clinical conundrum? Brit J Cardiol. 2009;16:281–6.

46. Engel GL, Farid NA, Faul MM, Richardson LA, Winneroski LL. Salt form selection and characterization of LY333531 mesylate monohydrate. Int J Pharm. 2000;198(2):239–47. https://doi.org/10.1016/s0378-5173(00)00350-1.

47. Furuta Y, Gowen BB, Takahashi K, Shiraki K, Smee DF, Barnard DL. Favipiravir (T-705), a novel viral RNA polymerase inhibitor. Antiviral Res. 2013;100(2):446–54. https://doi.org/10.1016/j.antiviral.2013.09.015.

48. Daikoku T, Mizuguchi M, Obita T, Yokoyama T, Yoshida Y, Takemoto M, et al. Characterization of susceptibility variants of poliovirus grown in the presence of favipiravir. J Microbiol Immunol Infect. 2018;51(5):581–6. https://doi.org/10.1016/j.jmii.2017.03.004.

49. Daikoku T, Yoshida Y, Okuda T, Shiraki K. Characterization of susceptibility variants of Influenza virus grown in the presence of T-705. J Pharmacol Sci. 2014;126(3):281–4. https://doi.org/10.1254/jphs.14156SC.

50. Sasaki-Tanaka R, Shibata T, Okamoto H, Moriyama M, Kanda T. Favipiravir inhibits Hepatitis A virus infection in human hepatocytes. Int J Mol Sci. 2022;23(5):2631. https://doi.org/10.3390/ijms23052631.